

Accepted Manuscript

Patched receptors sense, interpret and establish an epidermal Hedgehog signalling gradient

Christelle Adolphe, Jan Philipp Junker, Anna Lyubimova, Alexander van Oudenaarden, Brandon Wainwright

PII: S0022-202X(16)32238-2

DOI: [10.1016/j.jid.2016.06.632](https://doi.org/10.1016/j.jid.2016.06.632)

Reference: JID 478

To appear in: *The Journal of Investigative Dermatology*

Received Date: 18 October 2015

Revised Date: 1 June 2016

Accepted Date: 14 June 2016

Please cite this article as: Adolphe C, Junker JP, Lyubimova A, van Oudenaarden A, Wainwright B, Patched receptors sense, interpret and establish an epidermal Hedgehog signalling gradient, *The Journal of Investigative Dermatology* (2016), doi: 10.1016/j.jid.2016.06.632.

This is a PDF file of an unedited manuscript that has been accepted for publication. As a service to our customers we are providing this early version of the manuscript. The manuscript will undergo copyediting, typesetting, and review of the resulting proof before it is published in its final form. Please note that during the production process errors may be discovered which could affect the content, and all legal disclaimers that apply to the journal pertain.



Patched receptors sense, interpret and establish an epidermal Hedgehog signalling gradient

Christelle Adolphe^{1,4}, Jan Philipp Junker^{2,3,4}, Anna Lyubimova², Alexander van Oudenaarden² and Brandon Wainwright¹.

1. *Division of Molecular Genetics and Development, Institute for Molecular Bioscience, The University of Queensland, Brisbane, QLD 4072, Australia*
2. *Hubrecht Institute, KNAW and University Medical Centre Utrecht, 3584 CT Utrecht, the Netherlands.*
3. *Berlin Institute for Medical Systems Biology, Max Delbrück Center for Molecular Medicine; 13092 Berlin-Buch, Germany*
4. Co-first author

Correspondence: Brandon Wainwright, *Division of Genomics, Disease and Development, Institute for Molecular Bioscience, The University of Queensland, Brisbane, QLD 4072, Australia.* Email: b.wainwright@imb.uq.edu.au

Running title: An epidermal Hedgehog signalling gradient

Abbreviations: Hedgehog (Hh), hair follicle (HF), interfollicular epidermis (IFE), ligand-dependent antagonism (LDA), ligand-independent antagonism (LIA)

Abstract

By employing the sensitivity of single molecule fluorescent *in situ* hybridisation (smFISH) we have precisely quantified the levels and defined the temporal and spatial distribution of Hedgehog signalling activity during embryonic skin development, and uncovered that there is a Hedgehog signalling gradient along the proximal-distal axis of developing hair follicles. In order to explore the contribution of Hedgehog receptors Ptch1 and Ptch2 in establishing the epidermal signalling gradient, we quantitated the level of pathway activity generated in *Ptch1* and *Ptch1;Ptch2*-deficient skin and defined the contribution of each receptor to regulation of the levels of Hedgehog signalling identified in wild-type skin. Moreover, we show that both the cellular phenotype and level of pathway activity featured in *Ptch1;Ptch2*-deficient cells faithfully recapitulates the *Peak* level of endogenous Hedgehog signalling detected at the base of developing follicles, where the concentration of endogenous Shh is predicted to be highest. Taken together, these data demonstrate that both Ptch1 and Ptch2 play a crucial role in sensing the concentration of Hedgehog ligand and regulating the appropriate dose-dependent response.

Introduction

Precise temporal-spatial regulation of the Hedgehog (Hh) pathway activity is crucial to ensure normal development and prevent neoplastic transformation of cells in a number of diverse organs and tissues. Whilst the Hh pathway consists of a number of positive and negative regulators, the Patched (Ptch) protein receptors are perhaps the most important regulatory hub involved in the modulation Hh signalling. Ptch1 functions as a negative regulator of the pathway via two distinct processes. In the absence of Hh ligand, Ptch1 suppresses activity of the Smoothed (Smo) effector (Taipale *et al.*, 2002), a process referred to as ligand-independent antagonism (LIA) (Jeong and McMahon, 2005). Hedgehog ligands activate

signalling by binding to the Ptch1 receptor and inducing subsequent internalisation and lysosomal degradation of the Hh–Ptch complex (Incardona *et al.*, 2000), thereby allowing translocation of Smo to the tip of the primary cilium where it is phosphorylated into an active form (Corbit *et al.*, 2005) (Rohatgi *et al.*, 2007). Ptch1 itself is a transcriptional target of the pathway, a feedback mechanism that acts to increase the amount of Ptch1 protein available to further bind and deplete Hh ligand from the microenvironment. This mechanism of Hh sequestration acts to limit the field of pathway activity and ultimately attenuate the Hh signal, an effect called ligand-dependent antagonism (LDA) (Jeong and McMahon, 2005). Mammals also possess a paralogous Ptch receptor, Ptch2 (Motoyama *et al.*, 1998), however the role of Ptch2 has not been as comprehensively addressed as for Ptch1.

Constitutive Hh signalling activity is a characteristic feature of the common skin cancer, basal cell carcinoma (BCC). Mouse models simulating pathway activation via manipulation of Shh, Ptch1, Smo or Gli, lead to epidermal hyperplasia and formation of lesions resembling human BCC (see (Kasper *et al.*, 2012). A number of studies have been directed at dissecting the cellular origin of BCC, whereby Hh signalling activity has been activated in specific epidermal and HF stem/progenitor cell compartments. Despite these studies, the BCC-initiating cell compartment remains controversial and consensus has been difficult to attain with some studies reporting BCC formation following Hh activation in a variety of HF stem cell compartments (Grachtchouk *et al.*, 2011; Kasper *et al.*, 2011; Peterson *et al.*, 2015; Wang *et al.*, 2011), and others indicating BCC potential from IFE structures (Adolphe *et al.*, 2006; Grachtchouk *et al.*, 2011; Villani *et al.*, 2010; Wong and Reiter, 2011; Youssef *et al.*, 2012; Youssef *et al.*, 2010)

Aside from differences in the ascribed BCC cell of origin there is significant variation in the epidermal phenotypes of Hh pathway activation models, including: BCC potential, tumour latency and anatomical distribution of the lesions. We propose that variations in phenotype may reflect different amplitudes of Hh pathway activity in each model system. Previous studies by Dlugosz and colleagues (Grachtchouk *et al.*, 2003) have shown that the magnitude of Hh signalling activity defines the tumorigenic potential of the pathway. We have previously shown that loss of *Ptch1* activity is sufficient to induce BCC formation across all epidermal locations (Villani *et al.*, 2010). Thus the level of activity generated in *Ptch1*-deficient cells acts to define the tumorigenic threshold of Hh signalling in skin. In contrast, we have recently shown that concomitant inactivation of both *Ptch1* and *Ptch2* during epidermal development leads to loss of interfollicular epidermis (IFE), HF and sebaceous gland specification and differentiation (Adolphe *et al.*, 2014). Taken together, these data indicate that different amplitudes of Hh signalling activity drive distinct cellular responses and cell fate decisions in the skin.

In the developing neural tube, neuronal identity is defined by positional information generated by a *Shh* gradient. Recent methodology enabling quantification of Hh pathway transcriptional effectors has revealed that the amplitude of Hh signalling is critical in defining the gene expression profile and the ensuing cellular response (Cohen *et al.*, 2015; Junker *et al.*, 2014). To date, no Hh quantification studies have been performed in the skin, thus it remains unknown whether epidermal Hh signalling specifies different cell fate decisions in a manner akin to the neural tube. Here we utilise single molecule fluorescent *in situ* hybridisation (smFISH) to spatio-temporally quantitate *Ptch1* and *Gli1* mRNA transcription, as a read-out of Hh signalling activity and obtain precise quantification of epidermal Hh signalling in wild type, *Ptch1*-deficient and *Ptch1*;*Ptch2*-deficient skin. Consequently, we have defined both the

threshold of Hh pathway activity that leads to BCC formation and the amplitude of Hh signalling that specifies HF progenitor cells. In addition, our analyses of wild-type skin have identified a hitherto unrecognised proximal-distal Hh signalling gradient in developing hair follicles.

Results

Loss of *Ptch* receptor activity in the developing epidermis generates specific levels of Hedgehog pathway activity.

We recently proposed that the difference in outcome between a tumorigenic *Ptch1*-deficient phenotype and the loss of epidermal specification and differentiation observed in *Ptch1;Ptch2*-deficient skin is attributable to differences in the amplitude of Hh signalling activity subsequently evoking distinct cellular responses (Adolphe *et al.*, 2014). In order to define the amplitude of pathway activity we used single molecule fluorescent *in situ* hybridization (smFISH) to quantitate RNA transcript density of the Hh target genes *Ptch1* and *Gli1* in individual cells (Figure 1a) (Junker *et al.*, 2014; Raj *et al.*, 2008). Given follicular Hh pathway activity would confound the measurements attributable to loss of *Ptch*, we restricted our measurements to the interfollicular epidermis (IFE) region of each mouse model. In E17.5 wild-type epidermis few *Ptch1* (Figure 1b) and *Gli1* transcripts were detected in the IFE [*Ptch1*: 90% of cells <0.10 transcripts/ μm^3 (Figure 1b) and mean transcript density of 0.04/ μm^3 (Figure 1c); *Gli1*: 90% of cells <0.0125/ μm^3 (Figure 1b), mean transcript density of 0.006/ μm^3 (Figure 1c)]. Loss of *Ptch2* activity (*Ptch2*^{*tm1/tm1*}) resulted in levels of *Ptch1* and *Gli1* indistinguishable from control epidermis (data not shown).

Loss of *Ptch1* activity (*K5Cre:Ptch1^{lox/lox}*) drives moderate transcriptional activation of downstream target genes (Figure 1a) with an ~3-fold activation in *Ptch1* [90% of cells $<0.275/\mu\text{m}^3$ (Figure 1b) and mean transcript density of $0.11/\mu\text{m}^3$ (Figure 1c)] and ~4-fold activation in *Gli1* [90%: $<0.05/\mu\text{m}^3$ (Figure 1b), mean: $0.022/\mu\text{m}^3$ (Figure 1c)]. Consistent with our initial hypothesis, concomitant ablation of both *Ptch1* and *Ptch2* (*K5Cre:Ptch1^{lox/lox};Ptch2^{tm1/tm1}*) results in a greater level of pathway activation with *Ptch1* transcriptional activity in *Ptch1;Ptch2*-deficient cells (Figure 1a) being ~9-fold higher than control epidermis and ~3-fold higher than *Ptch1*-deficient cells [97% of cells $<0.65/\mu\text{m}^3$ (Figure 1b) and mean transcript density of $0.36/\mu\text{m}^3$ (Figure 1c)]. Similarly, *Gli1* transcription is dramatically amplified with an ~28-fold increase in transcriptional activation compared to that measured in wild-type IFE and ~7-fold increase over loss of *Ptch1* alone [5% of cells express WT reference ($<0.0125/\mu\text{m}^3$) and 15% expressing *Ptch1*-deficient reference levels ($<0.05/\mu\text{m}^3$) (Figure 1b) and mean transcript density of $0.16/\mu\text{m}^3$ (Figure 1c)]. Overall, these data clearly indicate that *Ptch2* plays a critical and substantial role in attenuating Hh pathway signalling in the absence of *Ptch1* LDA and LIA. In order to address whether the amplitude of Hh pathway activity generated in the *Ptch*-deficient skin mutants model properties of endogenous epidermal Hh signalling activity, we set out to define the temporal and spatial dynamics of Hh signalling and quantitate the amplitude of Hh-responsive cell populations in wild-type skin.

Hair follicles exhibit a proximal-distal Hedgehog signalling gradient

In contrast to the negligible level of *Ptch1* and *Gli1* in E17.5 wild-type IFE (Figure 1), we observed a proximal-distal distribution of *Ptch1* (Figure 2a) and *Gli1* in developing HF, highest at the proximal base and decreasing towards the IFE. Corresponding heat map intensity plots revealed three distinct levels of pathway activity in HF, with clear boundaries

demarcating each threshold (Figure 2b). We calculated that follicular cells residing in the uppermost third of the HF exhibit levels of mRNA transcript densities identical to IFE basal cells (Figure 2b: dark blue-heat map density). Follicular cells located in the central region of developing HFs exhibit a moderate measure of *Ptch1* transcriptional activation (ranging between $0.10/\mu\text{m}^3$ and $0.20/\mu\text{m}^3$) (Figure 2b: light blue-heat map density). In contrast, proliferating cells located at the base of the HF and actively invading the dermis, exhibit the greatest measure of *Ptch1* transcript density (ranging between $0.20/\mu\text{m}^3$ and $0.4/\mu\text{m}^3$) (Figure 2b: red heat map density). Numerically, the moderate amount of *Gli1* and *Ptch1* mRNA present in centrally located wild-type HF cells is directly comparable to the amplitude of pathway activity defined in *Ptch1*-deficient cells (Figure 1). Moreover, the greatest detected level of epidermal Hh signalling at the HF base is directly comparable to the amplitude of pathway activity defined in *Ptch1;Ptch2*-deficient cells (Figure 1).

In order to define the spatio-temporal distribution of Hh signalling activity during HF development we quantitated the *Ptch1* and *Gli1* transcript density along the proximal-distal length of HFs at different stages of the HF cycle. Previous studies have shown that Hh signalling is dispensable for HF initiation and hair germ development (stage 2) (Chiang *et al.*, 1999; St-Jacques *et al.*, 1998). Consistent with these findings, we observed low levels (90% $<0.10/\mu\text{m}^3$) of *Ptch1* mRNA in cells of the hair placode and hair germ (Figure 2c and d). Production of Shh ligand at the base of HFs as they transition between stage 2 and 3 (hair peg) results in an immediate and dramatic increase in *Ptch1* transcript density (90% $<0.35/\mu\text{m}^3$) (Figure 2f and g: red circle), directly comparable to the mean transcript density observed in *Ptch1;Ptch2*-deficient skin (Figure 1). As HFs proceed through each stage of maturation, the pool of cells located at the base of the HF continue to express the abundant *Ptch1* transcripts ($>0.20/\mu\text{m}^3$), equivalent to the amplitude of pathway activity defined in

Ptch1;Ptch2-deficient cells (2i and j: red circle). As the HF lengthens and cells become more distal to the Shh source, Hh signalling activity decreases (Figure 2g and j: blue arrow) to a threshold of signalling equivalent to that measured in *Ptch1*-deficient cells.

In order to address whether the developmental Hh signalling gradient persists in late stage anagen as the HF continues to lengthen and cells become even more distal to the Shh source, we screened P10 control skin. Akin to E17.5 HFs, we observed a proximal-distal gradient of *Ptch1* mRNA (Figure 2e) and corresponding heat map intensity plots reveal the persistence of three distinct levels of pathway activity (Figure 2l and m). These data show the maintenance of clear threshold boundaries throughout anagen growth.

Since *Ptch1;Ptch2*-deficient cells exhibit an equivalent amplitude of Hh signalling activity as the cells located at the base of wild-type HFs, we set out to determine whether the phenotype of *Ptch1;Ptch2*-deficiency is replicated in the corresponding endogenous cell population. One characteristic feature of *Ptch1;Ptch2*-deficient epidermal cells is loss of keratin 5 (K5) and K14 expression, indicating loss of epidermal basal cell fate and acquisition of a more primitive progenitor-like state (Adolphe *et al.*, 2014). Prior to Hh pathway activation all basal cells of E17.5 IFE and hair placode/germ exhibit K14 expression (Figure 2e). However, immediately upon Hh activation at the base of a hair peg, we observe a dramatic decrease in K14 expression (Figure 2h: red arrow). Indeed, cells during all stages of HF formation that express the greatest detected (*Ptch1;Ptch2*-deficient-like) measure of pathway activity present with a decrease in K14 expression (Figure 2k: red arrow). We observed a similar phenotypic correlation between HF cells expressing the greatest detected measure of pathway activity and *Ptch1;Ptch2*-deficiency using a number of other markers. For example, both *Ptch1;Ptch2*-deficient keratinocytes and wild-type follicular cells located in the HF bulb exhibit loss of

cell-cell adhesion. Cells presenting with K14 downregulation (Figure 3a, c, e and g) concurrently exhibit decreased e-cadherin (Figure 3b and f), p120-catenin (Figure 3d and h) and ZO-1 (data not shown) expression. These data further support the contention that *Ptch1;Ptch2*-deficiency results in an amplitude of Hh signalling activity that is recapitulated during normal epidermal development.

Discussion

The smFISH data described here have defined the spatio-temporal domains of Hh expression and defined the amplitudes of Hh activity in both wild-type and *Ptch* mutant epidermis. These data indicate that both *Ptch1* and *Ptch2* play an important role in sensing and establishing a previously unappreciated Hh signalling gradient in the skin.

Both *Ptch1* and *Ptch2* play an essential role in sensing and transducing the epidermal Hedgehog morphogen gradient

Our smFISH analyses have identified graded levels of Hh pathway activity emanating along the proximal-distal axis of developing HF (Figure 4a). We did not observe a spike in Hh pathway activity along the HF structure of embryonic HF. Hence, it is likely that the nerve fiber located at the upper bulge region, as described by (Brownell *et al.*, 2011), becomes a source of Hh ligand only in post-natal HF structures and is not a developmental source of Hh ligand. Here we show that keratinocytes located most distal from the *Shh* source, namely the IFE basal cell compartment and follicular cells located above the future HF bulge, exhibit an endogenously low *Basal* level of *Ptch1* and *Gli1* transcriptional activity (Figure 4a: dark blue colour scheme), likely due to a nominal concentration of ligand reaching this target field. In

contrast, follicular cells located between the future HF bulge and HF bulb exhibit elevated levels of *Ptch1* and *Gli1* transcriptional activity (Figure 4a: light blue colour scheme), consistent with their more proximal location to the Shh source and thus exposure to an intermediate concentration of ligand. Interestingly, the quantitated level of signalling activity within these centrally located HF cells is equivalent to the level of Hh activity measured in *Ptch1*-deficient cells. Given that *in vitro* studies have suggested Hh ligands display equivalent binding affinity to both Ptch1 and Ptch2 (Carpenter *et al.*, 1998), it is plausible that the magnitude of signalling activity in this wild-type HF location is generated by a ligand concentration that bind a proportion of available Ptch1 and Ptch2 receptors, resulting in loss of LIA and subsequent activation of the Smo effector. However, *Ptch1*-heterozygous;*Ptch2*-homozygous-deficient skin does not exhibit tumorigenic activity, clearly demonstrating that a half dose (single functioning allele) of Ptch1-LIA is sufficient to inhibit Smo activation. Thus it appears saturation of a majority of Ptch1 receptors is necessary to cross the *Basal* threshold and achieve physiological activation of the Hh pathway in wild-type skin.

We have also identified that the highest magnitude of Hh signalling activity established during epidermal development occurs in a small population of cells located at the base of wild-type developing HFs, in a structure referred to as the HF bulb (Figure 4a: red colour scheme). Given *Ptch1*;*Ptch2*-deficient keratinocytes exhibit an amplitude of pathway activity identical to cells of the HF bulb, it is likely that a concentration of ligand sufficiently high to saturate and internalize all available Ptch receptors is restricted to cells located within this target field (Figure 4a: RHS schematic). Taken together, these data indicate concomitant ablation of Ptch1 and Ptch2 is a genetic approach that mimics the biological program induced by the highest concentration of Shh in developing wild-type HFs (Figure 4c) and is a starting

point to ultimately dissect the molecular mechanisms involved in specification of this small endogenous population of progenitor-like cells.

Ptch1 and Ptch2 act synergistically to repress hedgehog pathway activity

We have previously shown that loss of Ptch1 alone is necessary and sufficient to induce basal cell carcinoma (BCC) formation (Adolphe *et al.*, 2006; Villani *et al.*, 2010). Here we have quantitated the level of Hh pathway activity generated in the IFE of *Ptch1*-deficient cells (K5Cre:*Ptch1*^{lox/lox}), and thus defined the tumour suppressor activity threshold of the Hh signalling pathway (Figure 4b: light blue dotted line). Several lines of evidence have indicated that BCC potential is only achieved upon what has been previously described as high (not intermediate or low) magnitudes of Hh signalling (Grachtchouk *et al.*, 2003), hence we term *Ptch1*-deficient cells as exhibiting a *High* level of Hh pathway activity (Figure 4: light blue colour scheme). In contrast, *Ptch1;Ptch2*-deficiency appears to simulate cells that are spatially located in the region of the HF bulb comprising multi-potent matrix progenitor cells. By calculating the threshold of transcriptional activity produced in *Ptch1;Ptch2*-deficient cells (K5Cre:*Ptch1*^{lox/lox};*Ptch2*^{tm1/tm1}) we have identified the level of Hh pathway signalling active in this pool of progenitor cells (Figure 4c: red dotted line). Genetic ablation of Ptch1 and Ptch2 results in ligand-independent, constitutive pathway activation downstream of Ptch repression (LIA). Complete de-repression of the pathway as modelled in *Ptch1;Ptch2*-deficient cells thus likely represents maximal Hh target gene transcription, which we define as a *Peak* level of signalling activity (Figure 4, red colour scheme).

It is predicted that *Ptch1;Ptch2*-deficient epidermis is not sensitive to Shh. Given Ptch1 and Ptch2 have been ablated, there is no means for a cell to detect, bind and interpret the presence of Shh ligand. However, in order to exclude the possibility that expansion of Shh ligand was

attributable to persistent *Peak* pathway activity throughout *Ptch1;Ptch2*-deficient epidermis, we screened for the distribution of *Shh*. Interestingly, *Shh* was not detectable by smFISH in *Ptch1;Ptch2*-deficient epidermis (Supplementary Figure 1). Given that all cells in *Ptch1;Ptch2*-deficient epidermis are genetically identical, it appears that *Shh* producing cells are not specified in response to *Peak* signaling activity. Moreover, it is important to note that we observed the histological phenotype of *Ptch1;Ptch2;Smo*-deficient epidermis is indistinguishable from that of *Smo*-deficient epidermis (Supplementary Figure 2), indicating *Peak* signalling is transduced via the canonical (Smo-dependent) pathway.

Peak signalling activity exhibits an approximate 3-fold (*Ptch1*) and 7-fold (*Gli1*) increase in transcript density when compared to *High* signalling activity. Given loss of *Ptch2* alone does not activate *Ptch1* or *Gli1* transcriptional activity, a substantial synergy exists between *Ptch1* LDA/LIA and *Ptch2* LDA/LIA in governing Hh pathway repression in the skin. The phenotype of complete pathway de-repression (*Ptch1;Ptch2*-deficiency) and whether *Ptch* synergism exists in other developmental systems remains to be determined. Recent reports describe the effects of *Ptch1;Ptch2* LDA ablation in the neural tube (Holtz *et al.*, 2013). However, these studies were performed in the presence of an MT-*Ptch1* transgene that ubiquitously expresses low levels of *Ptch*-LIA (Milenkovic *et al.*, 1999), and is therefore not representative of ligand-independent, constitutive pathway de-repression as described here.

Consistent with *Ptch1* playing an important role in sequestering Hh and limiting the diffusion of the ligand along a field of cells, we show that *Ptch1*-deficiency leads to an increased target field of *Peak* signalling towards the location of the HF bulge, culminating in a distal expansion of HF progenitor-like cells (Figure 4b). *Ptch1*-LIA is therefore crucial in preventing pathway tumorigenicity and *Ptch1*-LDA essential to restrict Hh signalling and

ensure appropriate proximal-distal HF cell fates. Similarly, we have identified *Ptch2* plays a vital role in establishing the epidermal Shh morphogen gradient and generating the Hh transcriptional code operating in actively growing HF progenitor cells.

Overall, our data suggest the availability of Ptch at the cell surface plays a critical role in regulating epidermal lineage specification, differentiation and proliferation by sensing the Shh morphogen gradient and defining whether a *Basal*, *High* or *Peak* transcriptional code is generated. The downstream targets specifying neoplastic transformation (*High*) or HF progenitor cell fate (*Peak*), and which ultimately define the boundaries between each epidermal gradient threshold remain to be determined. Although we postulate that the positive and negative regulators of Hh ligand upstream of Ptch (namely Cdo, Boc and Hhip) are unlikely to contribute or enhance the level of epidermal signaling following *Ptch1;Ptch2* ablation, further studies are warranted to identify whether they play a role in regulating the spatial distribution of transcription factors and demarcating the three distinct epidermal signaling thresholds defined here. However, it is clear that distinct levels of Hh signalling are associated with diverse biological responses. Thus dissecting the role of Hh pathway activity in normal organogenesis and disease requires a careful and quantitative consideration of pathway activity at the level of the individual cell.

Materials and Methods

K5Cre, *Ptch1* and *Ptch2* mice have been previously described (Adolphe *et al.*, 2014) and experiments performed according to the University of Queensland animal ethics guidelines. E18.5 flank skin samples were fixed in 4% PFA for 1 hour at 4°C, and incubated overnight in

30% sucrose at 4°C before embedding in OCT compound. Tissue blocks were sectioned at 8µm, postfixed in 4% PFA at room temperature for 15 minutes, rinsed in PBS and incubated overnight in 70% ethanol at 4°C. All experiments were performed in technical and biological replicates.

For each mRNA examined a set of 20-mer DNA oligonucleotides complementary to the coding region of the gene of interest were designed using an online program (<http://www.biosearchtech.com/stellarisdesigner/>) and synthesized with 3'-amino modifications by Biosearch Technologies. Probes were coupled to Alexa594 and Cy5 fluorophores as previously described (Lyubimova *et al.*, 2013). Tissue sections were hybridized as previously described (Lyubimova *et al.*, 2013; Raj *et al.*, 2008). Briefly, sections were hybridized with ~0.3 ng/µl of labelled probe sets for each mRNA overnight at 30°C in the dark. Sections were washed twice for 30 minutes and then mounted in anti-bleach buffer. Images were acquired on a Perking-Elmer Spinning Disc confocal microscope with a 100x oil-immersion objective (numerical aperture 1.4) using Perking Elmer Velocity software. Images were recorded as stacks with a z spacing of 0.3µm. Representative raw data images are shown in Figure 1a.

Diffraction-limited dots corresponding to single mRNA molecules were detected in 3D by custom Matlab software using previously described algorithms (Raj *et al.*, 2008). Briefly, the images were first filtered using a three-dimensional Laplacian of Gaussian filter with a width of 15 pixels and a standard deviation of 1.5 pixels. We then chose the intensity threshold at which the number of connected components was least sensitive to the threshold (Itzkovitz *et al.*, 2012). Individual images (tiles) were taken and stitched together in Matlab software (Raj *et al.*, 2008) using stage coordinates and cross-correlation analysis. Transcript density (units: #/µm³) was measured in pseudo cells of 5 µm x 5 µm size to generate 2D heat map plots.

Representative tiled data images are shown in Supplementary Figure 3. 1D transcript density traces were generated by plotting the mean value in sliding windows along the posterior-distal axis of a developing HF. Colored patches designate the standard deviation across pseudo cells.

Conflict of interest

The authors declare no conflict of interests.

Acknowledgements

Work in BW's laboratory was supported by research grants from the Australian Research Council (ARC) and National Health and Medical Research Council of Australia Project Grant 517948. Work in AvO's laboratory was supported by a European Research Council Advanced grant (ERC- AdG 294325-GeneNoiseControl) and by a Nederlandse Organisatie voor Wetenschappelijk Onderzoek (NWO) Vici award.

References

- Adolphe C, Hetherington R, Ellis T, Wainwright B (2006) Patched1 functions as a gatekeeper by promoting cell cycle progression. *Cancer Res* 66:2081-8.
- Adolphe C, Nieuwenhuis E, Villani R, Li ZJ, Kaur P, Hui CC, *et al.* (2014) Patched 1 and patched 2 redundancy has a key role in regulating epidermal differentiation. *J Invest Dermatol* 134:1981-90.
- Brownell I, Guevara E, Bai CB, Loomis CA, Joyner AL (2011) Nerve-derived sonic hedgehog defines a niche for hair follicle stem cells capable of becoming epidermal stem cells. *Cell Stem Cell* 8:552-65.
- Carpenter D, Stone DM, Brush J, Ryan A, Armanini M, Frantz G, *et al.* (1998) Characterization of two patched receptors for the vertebrate hedgehog protein family. *Proc Natl Acad Sci U S A* 95:13630-4.
- Chiang C, Swan RZ, Grachtchouk M, Bolinger M, Litingtung Y, Robertson EK, *et al.* (1999) Essential role for Sonic hedgehog during hair follicle morphogenesis. *Dev Biol* 205:1-9.
- Cohen M, Kicheva A, Ribeiro A, Blassberg R, Page KM, Barnes CP, *et al.* (2015) Ptch1 and Gli regulate Shh signalling dynamics via multiple mechanisms. *Nat Commun* 6:6709.
- Corbit KC, Aanstad P, Singla V, Norman AR, Stainier DY, Reiter JF (2005) Vertebrate Smoothed functions at the primary cilium. *Nature* 437:1018-21.
- Grachtchouk M, Pero J, Yang SH, Ermilov AN, Michael LE, Wang A, *et al.* (2011) Basal cell carcinomas in mice arise from hair follicle stem cells and multiple epithelial progenitor populations. *J Clin Invest* 121:1768-81.
- Grachtchouk V, Grachtchouk M, Lowe L, Johnson T, Wei L, Wang A, *et al.* (2003) The magnitude of hedgehog signaling activity defines skin tumor phenotype. *The EMBO journal* 22:2741-51.
- Holtz AM, Peterson KA, Nishi Y, Morin S, Song JY, Charron F, *et al.* (2013) Essential role for ligand-dependent feedback antagonism of vertebrate hedgehog signaling by PTCH1, PTCH2 and HHIP1 during neural patterning. *Development* 140:3423-34.
- Incardona JP, Lee JH, Robertson CP, Enga K, Kapur RP, Roelink H (2000) Receptor-mediated endocytosis of soluble and membrane-tethered Sonic hedgehog by Patched-1. *Proc Natl Acad Sci U S A* 97:12044-9.
- Jeong J, McMahon AP (2005) Growth and pattern of the mammalian neural tube are governed by partially overlapping feedback activities of the hedgehog antagonists patched 1 and Hhip1. *Development* 132:143-54.
- Junker JP, Peterson KA, Nishi Y, Mao J, McMahon AP, van Oudenaarden A (2014) A predictive model of bifunctional transcription factor signaling during embryonic tissue patterning. *Dev Cell* 31:448-60.

- Kasper M, Jaks V, Are A, Bergstrom A, Schwager A, Barker N, *et al.* (2011) Wounding enhances epidermal tumorigenesis by recruiting hair follicle keratinocytes. *Proc Natl Acad Sci U S A* 108:4099-104.
- Kasper M, Jaks V, Hohl D, Toftgard R (2012) Basal cell carcinoma - molecular biology and potential new therapies. *J Clin Invest* 122:455-63.
- Lyubimova A, Itzkovitz S, Junker JP, Fan ZP, Wu X, van Oudenaarden A (2013) Single-molecule mRNA detection and counting in mammalian tissue. *Nat Protoc* 8:1743-58.
- Milenkovic L, Goodrich LV, Higgins KM, Scott MP (1999) Mouse patched1 controls body size determination and limb patterning. *Development* 126:4431-40.
- Motoyama J, Takabatake T, Takeshima K, Hui C (1998) Ptch2, a second mouse Patched gene is co-expressed with Sonic hedgehog. *Nat Genet* 18:104-6.
- Peterson SC, Eberl M, Vagnozzi AN, Belkadi A, Veniaminova NA, Verhaegen ME, *et al.* (2015) Basal cell carcinoma preferentially arises from stem cells within hair follicle and mechanosensory niches. *Cell Stem Cell* 16:400-12.
- Raj A, van den Bogaard P, Rifkin SA, van Oudenaarden A, Tyagi S (2008) Imaging individual mRNA molecules using multiple singly labeled probes. *Nat Methods* 5:877-9.
- Rohatgi R, Milenkovic L, Scott MP (2007) Patched1 regulates hedgehog signaling at the primary cilium. *Science* 317:372-6.
- St-Jacques B, Dassule HR, Karavanova I, Botchkarev VA, Li J, Danielian PS, *et al.* (1998) Sonic hedgehog signaling is essential for hair development. *Current biology : CB* 8:1058-68.
- Taipale J, Cooper MK, Maiti T, Beachy PA (2002) Patched acts catalytically to suppress the activity of Smoothened. *Nature* 418:892-7.
- Villani RM, Adolphe C, Palmer J, Waters MJ, Wainwright BJ (2010) Patched1 inhibits epidermal progenitor cell expansion and basal cell carcinoma formation by limiting Igfbp2 activity. *Cancer Prev Res (Phila)* 3:1222-34.
- Wang GY, Wang J, Mancianti ML, Epstein EH, Jr. (2011) Basal cell carcinomas arise from hair follicle stem cells in Ptch1(+/-) mice. *Cancer Cell* 19:114-24.
- Wong SY, Reiter JF (2011) Wounding mobilizes hair follicle stem cells to form tumors. *Proc Natl Acad Sci U S A* 108:4093-8.
- Youssef KK, Lapouge G, Bouvree K, Rorive S, Brohee S, Appelstein O, *et al.* (2012) Adult interfollicular tumour-initiating cells are reprogrammed into an embryonic hair follicle progenitor-like fate during basal cell carcinoma initiation. *Nat Cell Biol* 14:1282-94.
- Youssef KK, Van Keymeulen A, Lapouge G, Beck B, Michaux C, Achouri Y, *et al.* (2010) Identification of the cell lineage at the origin of basal cell carcinoma. *Nat Cell Biol* 12:299-305.

Figure Legends

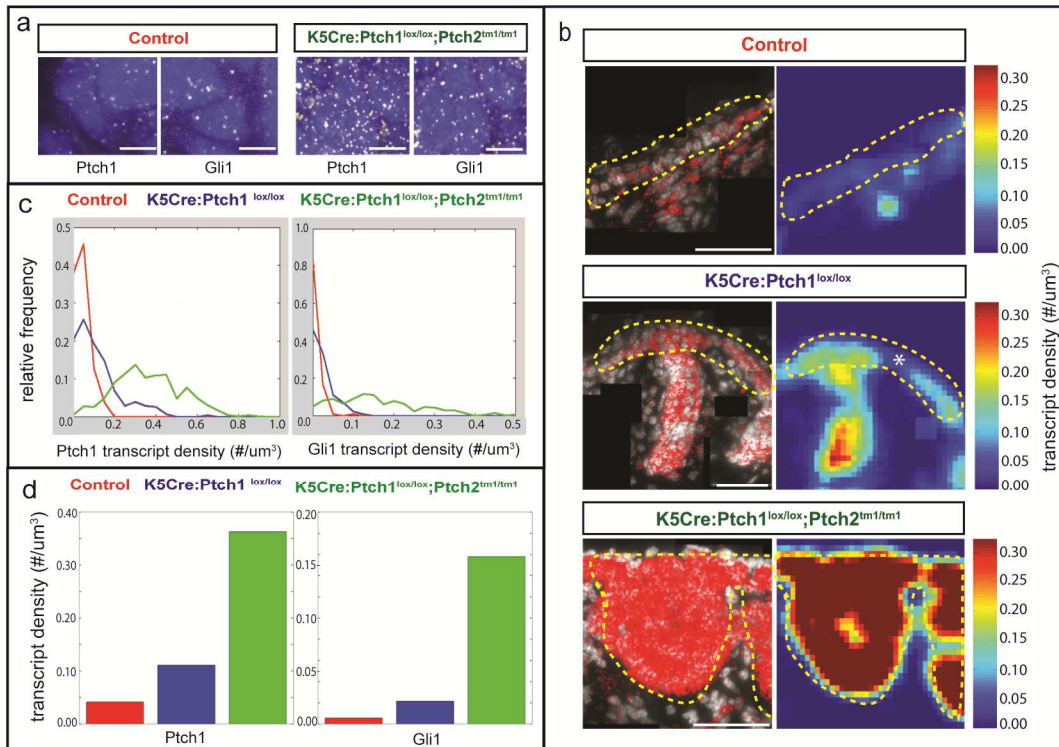
Figure 1: Quantitation of Hedgehog pathway activity in wild-type and *Patched*-deficient basal cells epidermis a) Maximum z projections (thickness 1.5 μ m) of smFISH raw data in control and *Ptch1*;*Ptch2*-deficient keratinocytes. Dapi nuclear stain shown in blue. Scale bar 5 μ m. b) Detected transcripts and corresponding heat maps showing abundance of *Ptch1* mRNA in E17.5 control, *Ptch1*-deficient and *Ptch1*;*Ptch2*-deficient epidermis. Analyses were restricted to the interfollicular basal cell compartment (yellow dotted regions). Scale bar 50 μ m. c) Quantitation of *Ptch1* and *Gli1* transcript density distribution and d) Mean transcript levels in E17.5 control (red), *Ptch1*-deficient (blue) and *Ptch1*;*Ptch2*-deficient (green) cells. * lower signal attributable to a fold in the IFE, hence reduced cell density available for calculation.

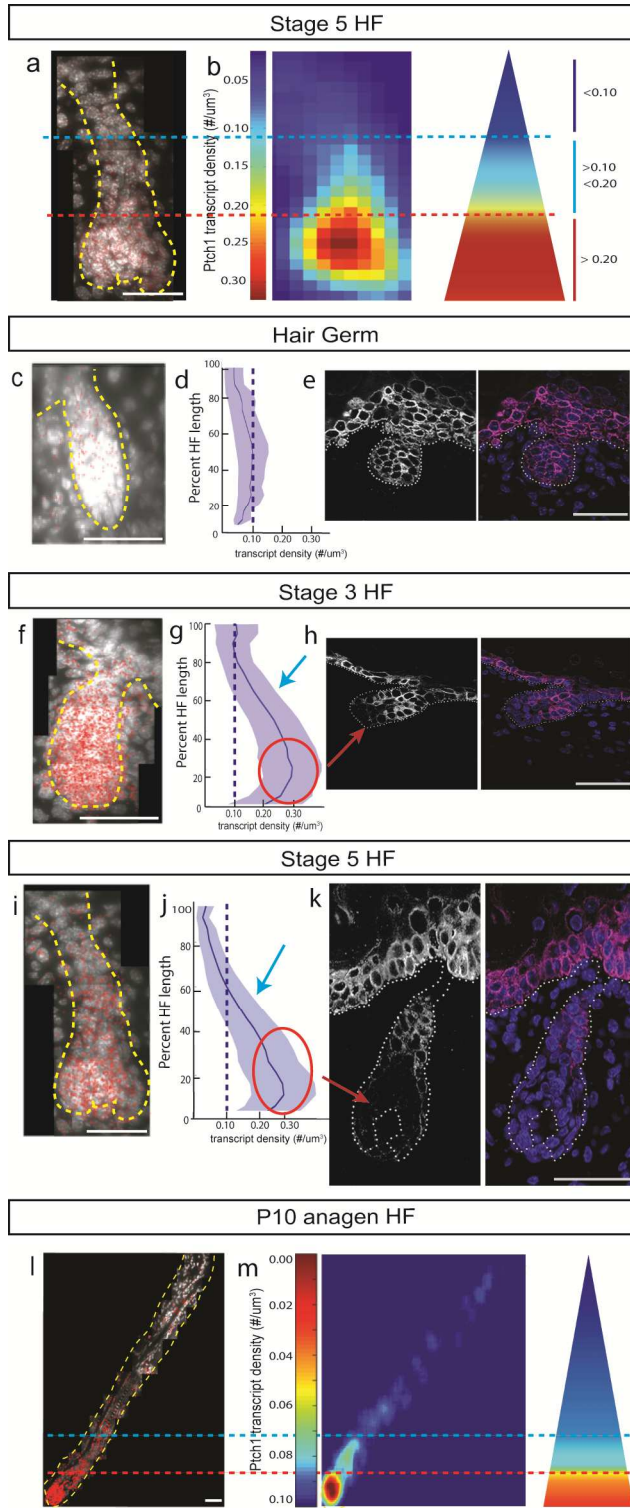
Figure 2: Hedgehog pathway activity in embryonic hair follicles. a) Detected transcripts and b) corresponding heat map showing the spatial abundance of *Ptch1* mRNA along the posterior-distal axis of aE17.5 developing HF. Note: three detectable levels of Hh pathway activity in embryonic HF. c) Low levels of *Ptch1* transcription are detected in early stage hair germs. d) Mean transcript density as a function of HF length. Shaded area corresponds to standard deviation. e) K14 is expressed in all keratinocytes of the hair germ. f) The Hh pathway becomes active in a stage 3 HF, with g) abundant *Ptch1* transcripts (>0.20 transcript density/ μm^3) occurring in the proximal keratinocytes of the hair peg (red circle), concomitant with h) loss of K14 protein expression (red arrow). i and j) Abundantly Hh-responsive cells remain localised to the proximal tip (red circle) of further developed (Stage 5) HF. k) Loss of K14 protein observed in cells exhibiting abundant *Ptch1* transcripts (>0.20 transcript density/ μm^3) (red arrow). l) Detected transcripts and m) corresponding heat map showing the

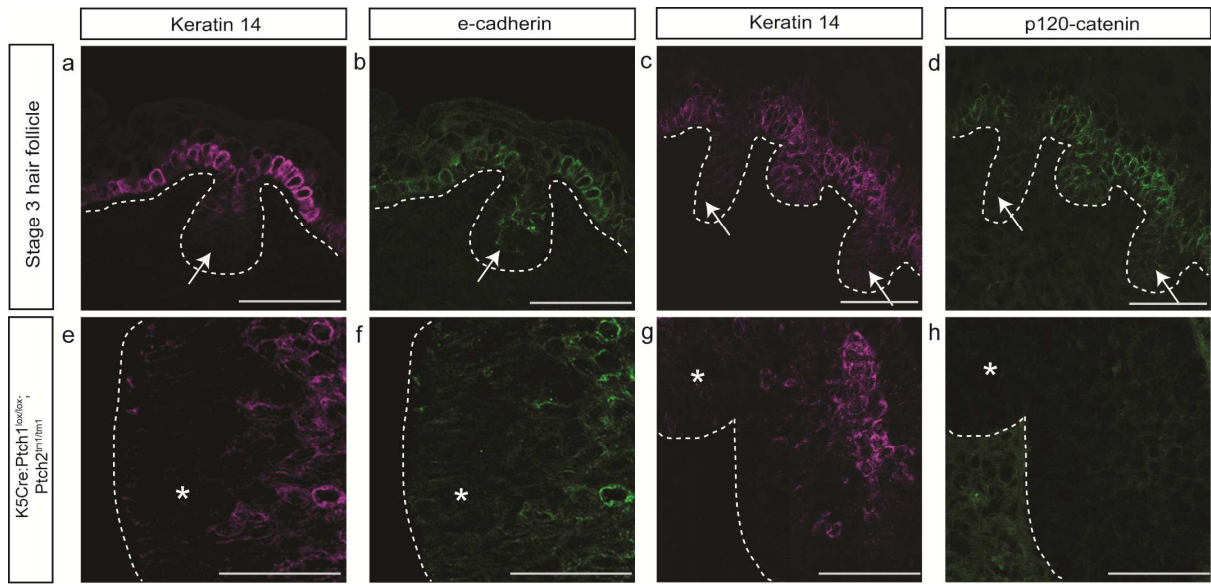
spatial abundance of *Ptch1* mRNA along the posterior-distal axis of a late stage anagen (P10) HF. Note: three detectable levels of Hh pathway activity in P10 HFs. Scale bar 50 μ m. IFE: interfollicular epidermis, HF: hair follicle, K14: keratin 14

Figure 3: Parallel protein expression profile in proximal HF and *Ptch1*;*Ptch2*-deficient cells. Concomitant loss of a) K14 and b) e-cadherin in E18.5 developing HFs (arrows). Concomitant loss of c) K14 and d) p120-catenin in E16.5 developing HFs (arrows). Concomitant loss of e) K14 and f) e-cadherin in E18.5 *Ptch1*;*Ptch2*-deficient keratinocytes (asterisk). Concomitant loss of g) K14 and h) p120-catenin in E18.5 *Ptch1*;*Ptch2*-deficient keratinocytes (asterisk). Scale bar 50 μ m.

Figure 4: Model for the regulation of epidermal morphogen signalling via Patched activity. a) Diagrammatic representation of the Hedgehog signalling gradient present in developing HFs. Three distinct levels of hedgehog signalling (indicated by colour), illustrated here as abundance of *Gli1* transcript. Middle panel: correlation between level of pathway activity and cell fate specification along the proximal-distal axis of the HF. RHS panel: proposed model of *Ptch* receptor saturation along the HF gradient. b) Loss of *Ptch1* receptor activity results in distal expansion of *High* and *Peak* levels of Hh activity. Blue dotted line: denotes threshold attributable to tumour formation. Loss of *Ptch1*-LDA results in decreased ligand sequestration leading to an increased range of ligand diffusion, thereby affecting the demarcation of standard threshold boundaries. c) *Ptch1* and *Ptch2* receptor saturation results in cell autonomous, constitutive *Peak* activity. Scale bar 50 μ m.







ACCEPTED MANUSCRIPT

